Water Resources Research

Supporting Information for

Factors determining the natural fresh-salt groundwater distribution in deltas

J. van Engelen[1,2], M.F.P. Bierkens[1,2], J.R. Delsman[2], G.H.P. Oude Essink[1,2]

[1]Department of Physical Geography, Utrecht University, Utrecht.

[2]Unit of Subsurface & Groundwater Systems, Deltares, Utrecht.

Corresponding author: Joeri van Engelen (joeri.vanengelen@deltares.nl)

Contents of this file

Introduction

This supporting information includes additional model support and information. Text S1 provides additional explanation on how the synthetic delta is constructed. Text S2 shows the mathematical derivation of an equation to correct the salinity intrusion length in surface water for a changing hydraulic gradient. Figure S1 shows that a linear salinity profile in the river system is sufficient model for this study. Figure S2 shows the effect of changing the horizontal aquifer hydraulic conductivity in 10 trajectories. Table S1 shows the inputs that were fixed in the sensitivity analysis.

Text S1. Additional explanation to model geometry, lithology, and boundary conditions

The geometry of the synthetic delta aquifer was created by specifying a set of inputs over three planes. Two of these planes (Fig. 1a & 1c) were in polar coordinates (r, ϕ) and the third plane (Fig. 1b) was consequently used to convert these to a cartesian coordinate system (x, y). First, the geometry was determined along the rz-plane (Fig. 1a), a cross-section from delta apex to the coast through the delta center. By connecting the depth specified at the apex (H_a) and at the coast (H_b) the hydrogeological base at ϕ=0, $\boldsymbol{z_{center}}$, was drawn and extrapolated until it intersected the top of the aquifer at the coastal slope. Furthermore, we specified the shape along the xy-plane by creating a sector ("pizza slice") with angle φ_f (Fig. 1b). To complete the geometry of the hydrogeological base, the depth across the ϕz-plane $\boldsymbol{z_{base}}$ was calculated as a half-ellipse (Fig. 1c) by inserting $\boldsymbol{z_{center}}$ as z in:

$$z_{ellipse}(z, \varphi) = \frac{z}{\varphi_f}\sqrt{\varphi_f^2 - \varphi^2} \qquad (S1.1)$$

For the lithology of the delta, we distinguished between the Holocene confining clay layer and the other pre-Holocene aquitards. A set of N_{aqt} aquitards was created that had the following thickness d_{clay}:

$$d_{\text{clay}} = \frac{f_{aqt} * \boldsymbol{z_{center}}}{N_{aqt} + 1} \qquad (S1.2)$$

where f_{aqt} is fraction of the sediment column that is aquitard. These N_{aqt} aquitards curved downward across the φz-plane (Fig. 1g) and dip downward in the coastal direction of the rz-plane (Fig. 1e), by calculating:

$$\boldsymbol{z_{clay,i}} = \left(\frac{i}{N_{aqt} + 1}\right) \cdot \left(\frac{\boldsymbol{z_{center}} + \boldsymbol{z_{base}}}{2}\right) \qquad (S1.3)$$

with $i = 1 \ldots N_{aqt}$

This confining layer had one additional input, l_{conf} that set its onshore extent (Fig. 1f). Beyond this point, the confining layer had zero thickness. The thickness of the confining layer was consequently calculated by calculating the thickness at the coast with equation 2, and linearly interpolating this with respect to l_{conf}.

The location of the coast was specified as follows. We call the location and moment of maximum transgression respectively r_{tra} and t_{tra} (Fig. 2c). To arrive at a smooth transition from the point where sea level equals the topography $r_{sea=top}$ to r_{tra}, we introduce the following equations:

$$r_{coast} = l_a L(1 - l_{tra})w + r_{sea=top}(1 - w) \qquad (S1.4)$$

where l_a is the relative length of the onshore, L the total length of the onshore, which we set to 200 km, l_{tra} the relative length of onshore covered with sea water at t_{tra}, and w as a weighting factor which is defined as:

$$w = \begin{cases} 0 & t < t_{start} \\ \dfrac{t - t_{start}}{t_{tra} - t_{start}} & t_{start} > t >= t_{tra} \\ \dfrac{t - t_{tra}}{t_{end} - t_{tra}} & t_{tra} < t < t_{end} \end{cases} \qquad (S1.5)$$

with t_{start} as the start of the Holocene and t_{end} as the present day ($t = 0$ ka).

Text S2. Support for choice linear salinity profile onshore surface waters and its correction factor based on river gradients

To reduce the amount of inputs in our global sensitivity analysis, a simple linear model was fitted to Savenije's model (2012), based on l_{surf}. Figure S1.1 shows that the fit of this simplification to the original model is in most cases satisfactory, from which we conclude that the linear salinity profile is sufficient to observe the effect of salinity intrusion on the groundwater salinity.

We correct the salinity intrusion length l_{surf} for each stress period to incorporate the effect of the large changes in river gradient as follows. Firstly, a river gradient correction factor f_i is defined.

$$\frac{i}{i_{end}} = \frac{f_i}{f_{i,end}} \qquad (S2.1)$$

Where i is the river gradient at any moment in time, i_{end} is the river gradient at 0 ka (which is equal to the topography (α) in our model setup), and $f_{i,end} = 1$, the correction factor for the last timestep. The reason why we explicitly define this last factor is shown hereafter in equation S1.7. The Chezy formula is defined as (eq 2.5.5 in Chow et al., 1988):

$$Q_{f,riv} = A_{riv} C \sqrt{R_{riv}\, i} \qquad (S2.2)$$

Where $Q_{f,riv}$ is the fresh water flow of the river, C is the Chezy constant, R_{riv} the hydraulic radius and A_{riv} the cross-sectional area. Savenije's equation for the salinity intrusion length in estuaries l_{surf} is (eq. 5.48 in Savenije, 2012):

$$l_{surf} = l_{con} \ln\left(\frac{1}{\delta} + 1\right) \qquad (S2.3)$$

Where l_{con} is the cross-sectional convergence length and δ is the tidal dispersion reduction rate (eq. 5.47 in Savenije, 2012):

$$\delta = \frac{B\, l_{con}\, Q_{f,riv}}{D_{mouth} A_{mouth}} \qquad (S2.4)$$

Where B is the van der Burgh coefficient, and D_{mouth} and A_{mouth} respectively are the longitudinal tidal dispersion and the cross-sectional surface area at the estuary mouth.

$Q_{f,riv}$ is governed by the climate and is assumed constant, so the higher velocities due to an increase in i would lead to a decrease in A_{riv}, which we assume to be proportional to the decrease in A_{mouth} this would also result in, leading to:

$$\frac{\frac{1}{A_{mouth}}}{\frac{1}{A_{mouth,end}}} = \frac{\sqrt{f_i}}{\sqrt{f_{i,end}}} \qquad (S2.5)$$

Subsequently assuming only A_{mouth} is not constant over time in S1.4, we can substitute S1.5 into S1.4, yielding:

$$\frac{\delta}{\delta_{end}} = \frac{\sqrt{f_i}}{\sqrt{f_{i,end}}} \tag{S2.6}$$

Which can then be consequently used to correct l_{surf} by substituting S1.6 into S1.3 (as a reminder $f_{i,end} = 1$):

$$\frac{l_{surf}}{l_{surf,end}} = \frac{\ln\left(\frac{1}{\sqrt{f_i}} + 1\right)}{\ln\left(\frac{1}{\sqrt{f_{i,end}}} + 1\right)} = \frac{\ln\left(\frac{1}{\sqrt{f_i}} + 1\right)}{\ln(2)} \tag{S2.7}$$

Since $f_{i,end} = 1$ and $i_{end} = \alpha$ in our model setup, we can substitute S1.1 into S1.7, yielding the intrusion length correction factor f_l:

$$f_l = \frac{l_{surf}}{l_{surf,end}} = \frac{\ln\left(\frac{1}{\sqrt{\frac{i}{\alpha}}} + 1\right)}{\ln(2)} \tag{S2.8}$$

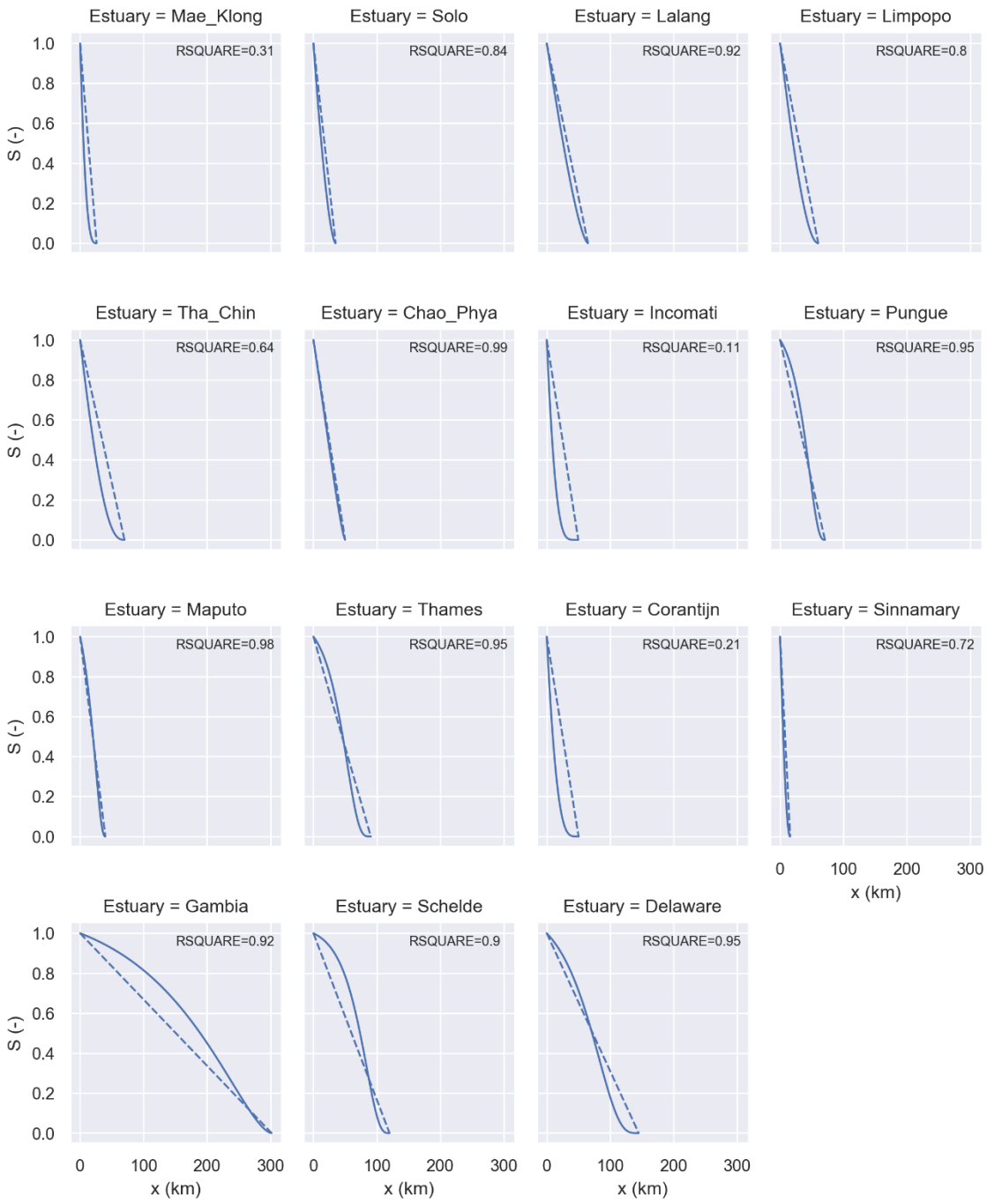

Figure S1. Fits of a linear model to the more advanced salinity intrusion models of Savenije (2012). *x* is the length landwards, *S* is the relative salinity. *S* = 1 is sea salinity, *S* = 0 is fresh water salinity. Inputs for all estuaries are from the mentioned source.

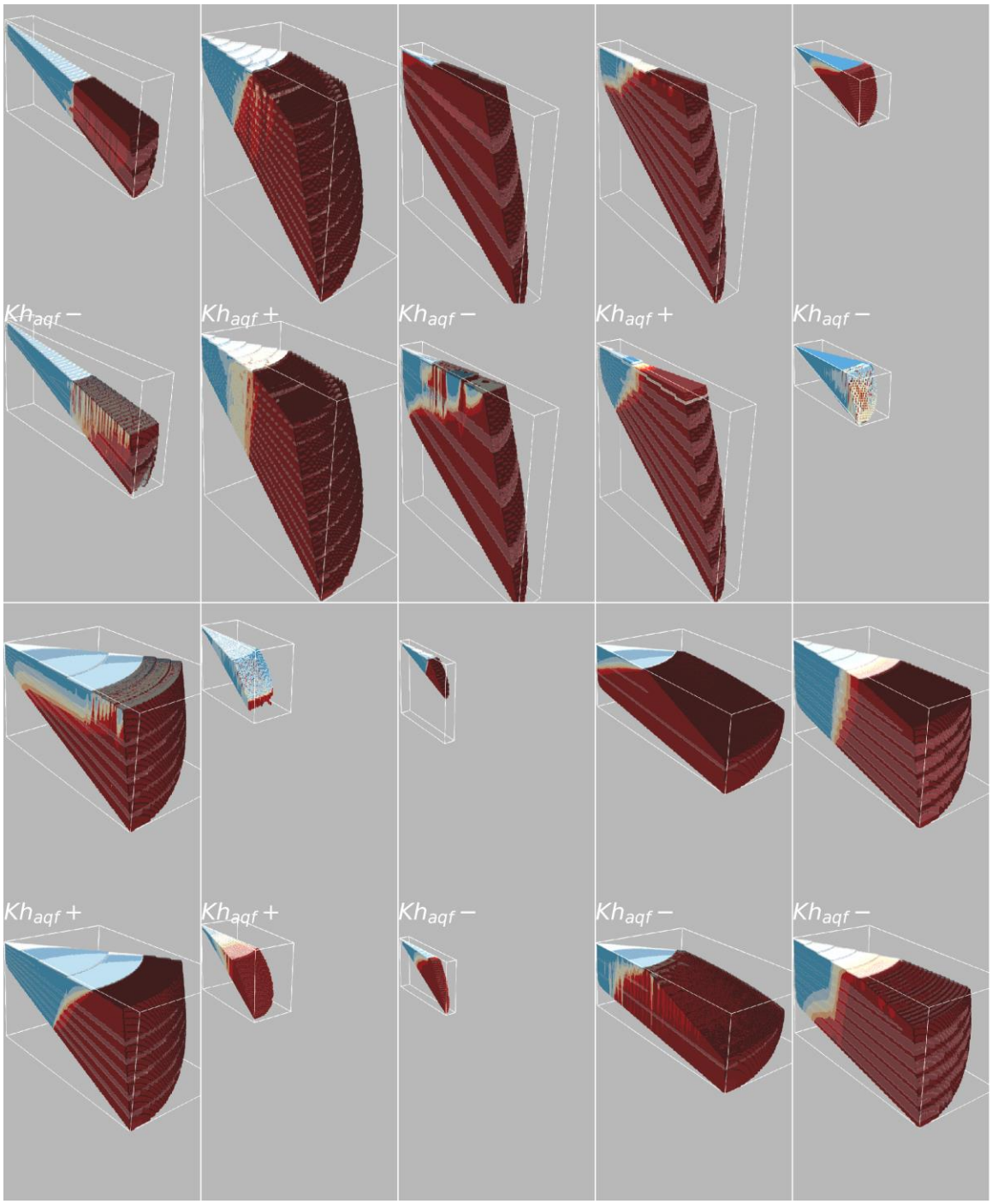

Figure S2: Effects of changes of $K_{h,aqf}$ on the fresh-salt distribution for ten trajectories. The bottom figure in each panel presents the effect of change in $K_{h,aqf}$. The sign designates if $K_{h,aqf}$ is increased (+) or decreased (-). The colors indicate the salinity: red is saline, yellow is brackish, and blue is fresh. A lighter shade of color indicates a clay layer. Note that the vertical of each distribution with the following is stretched by a factor $4000/\sqrt{\Delta z}$, since the system thickness varied logarithmically.

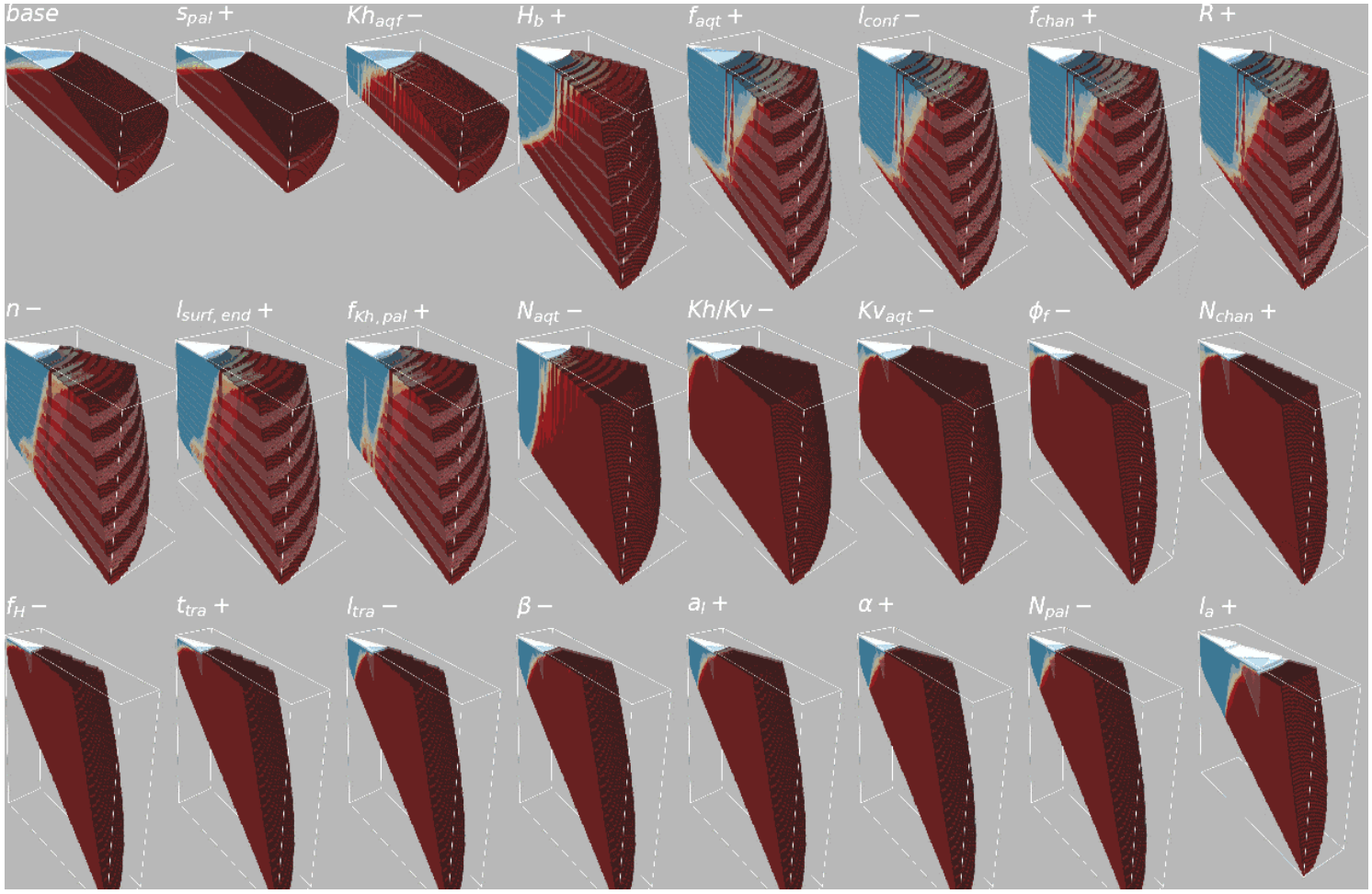

Figure S3: End-state results of one trajectory. The symbol indicates the input that is changed, the sign whether this input is increased or decreased. The trajectory starts at the top left, and goes from left to right, top to bottom. “Base” indicates the starting point. The white zone on top indicates the onshore part of the domain, the black part the offshore. The dark red colors indicate saline groundwater, the yellow colors brackish, and the blue colors indicate fresh groundwater.

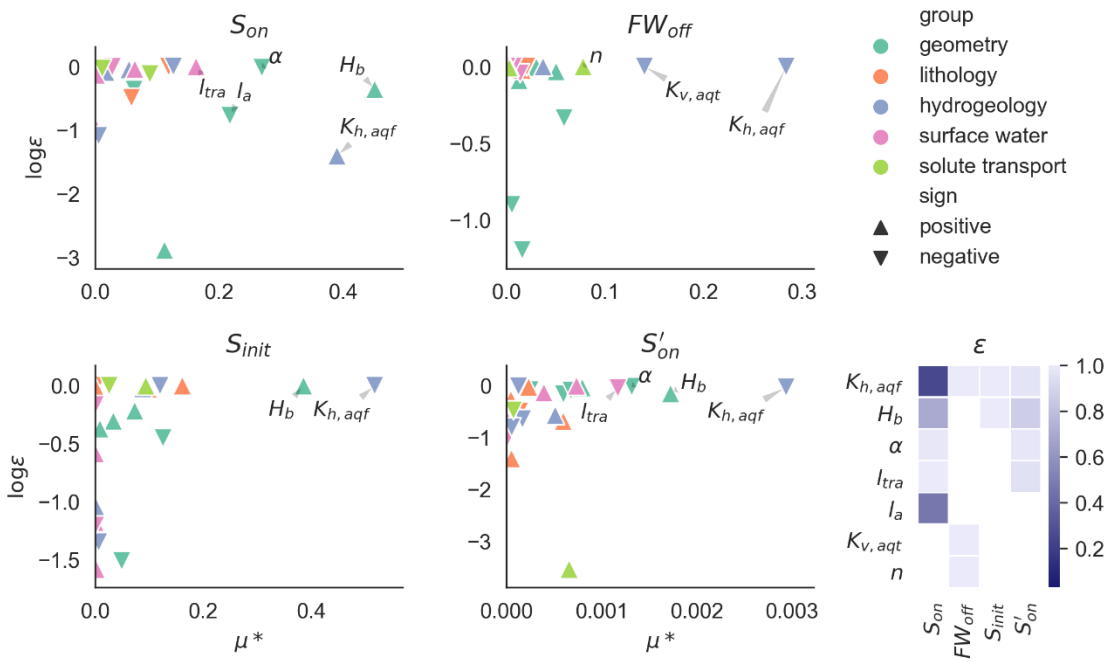

Figure S4: Scatter plots of the mean absolute elementary effect (μ^*) against the logarithm of the monotonicity (ε) of each input for the four metrics (S_{on}, FW_{off}, S_{init}, S'_{on}). Each input is represented by a triangle, the orientation of which indicates whether the input has a positive effect on the metric or not. The colors indicate the group the inputs belong to in Table 1. The labeled inputs are the most sensitive.

Table S1. Fixed inputs in the global sensitivity analysis

Symbol	Description	Value	Unit	Reference
		Morris		
N_{lev}	Number of levels	4	-	(Morris, 1991)
N_{traj}	Number of trajectories	10	-	(Khare et al., 2015)
N_{inp}	Number of inputs	23	-	Table 1
		Geometry		
γ	Angle coastal slope	2.5e-2	rad	(GEBCO, 2014)
L	Absolute total extent delta	200	km	Section 2.1 main article
		Hydrogeology		
S_s	Specific storage	6.3e-5	1/d	Mean value of data review
		Surface water		
rs_{surf}	Resistance surface waters	10	d	Assumed
C_f	Concentration fresh water.	0	g TDS/l	Assumed
C_s	Concentration sea water.	35	g TDS/l	(Millero, 2010)
		Solute transport		
a_t/a_l	Ratio of transversal over longitudinal dispersion length	1e-1	-	(Gelhar et al., 1992)
a_v/a_l	Ratio of vertical over longitudinal dispersion length	1e-2	-	(Gelhar et al., 1992)
D_m	Molecular diffusion coefficient	8.64e-5	m^2/d	(Guo & Langevin, 2002)
$\partial\rho/\delta C$	Linear density conversion slope	0.7143	$\frac{\text{g TDS/l}}{\text{kg/m3}}$	(Kohfahl et al., 2015)